

## IN VITRO EVALUATION OF FRACTURE RESISTANCE OF VARIOUS THICKNESS FIBER-REINFORCED COMPOSITE INLAY FPD

Yang-Jin Yi<sup>1</sup>, D.D.S., M.S.D., Ph.D., Dong-Jin Yoon<sup>2</sup>, M.S., Ph.D.,  
Chan-Jin Park<sup>1</sup>, D.D.S., M.S.D., Ph.D., Lee-Ra Cho<sup>1</sup>, D.D.S., M.S.D., Ph.D.

<sup>1</sup>Dept. of Prosthodontics, College of Dentistry, Kangnung National University,  
and Reséarch Institute of Oral Science

<sup>2</sup>NDE Lab., Korea Research Institute of Standards and Science

**Statement of problem.** In dentistry, the minimally prepared inlay resin-bonded fixed partial denture (FPD) made of new ceromer / fiber-reinforced composite (FRC) was recently introduced. However, the appropriate dimensions for the long-term success and subsequent failure strength are still unknown.

**Purpose.** The aim of this study was to investigate the most fracture-resistible thickness combination of the ceromer / FRC using a universal testing machine and an AE analyzer.

**Material and Methods.** A metal jig considering the dimensions of premolars and molars was milled and 56-epoxy resin dies, which had a similar elastic modulus to that of dentin, were duplicated. According to manufacturer's instructions, the FRC beams with various thicknesses (2 to 4 mm) were constructed and veneered with the 1 or 2 mm-thick ceromers. The fabricated FPDs were luted with resin cement on the resin dies and stored at room temperature for 72 hours. AE (acoustic emission) sensors were attached to both ends, the specimens were subjected to a compressive load until fracture at a crosshead speed of 0.5 mm/min. The AE and failure loads were recorded and analyzed statistically.

**Results.** The results showed that the failure strength of the ceromer / FRC inlay FPDs was affected by the total thickness of the connectors rather than the ceromer to FRC ratio or the depth of the pulpal wall. Fracture was initiated from the interface and propagated into the ceromer layer regardless of the change in the ceromer / FRC ratio.

**Conclusion.** Within the limitations of this study, the failure loads showed significant differences only in the case of different connector thicknesses, and no significant differences were found between the same connector thickness groups. The application of AE analysis method in a fiber-reinforced inlay FPD can be used to evaluate the fracture behavior and to analyze the precise fracture point.

### Key Words

Fiber-Reinforced Composite, Inlay FPD, Thickness, Fracture, AE

※ This work was supported by grant No. 2002-0249 from the Kangnung National University Hospital.

Inlay fixed partial denture (FPD) is useful for restoring single posterior missing teeth, especially for the abutment an existing old restoration, with a reduced invasiveness and better esthetics. However, the initial cast metal framework inlay FPD showed a loss of adhesion at the metal cement interface derived from the different elastic modulus between the abutment and the metal.<sup>1</sup> More esthetic all ceramic materials have been tried to posterior inlay FPD experimentally,<sup>2,3</sup> but these materials have own brittleness and are subject to failure.

The ceromer / fiber-reinforced composite (FRC) is an adequate material for restoring an inlay FPD with the characteristics of a metal-free translucency, good handling characteristics and a high flexure strength.<sup>4</sup> Behr et al.<sup>5</sup> demonstrated the possibilities applying a ceromer / FRC to restore the posterior region using in-vitro experiment in which an inlay FPD made of a ceromer / FRC showed a failure strength of approximately 700 N. Some clinical reports stated that a ceromer / FRC could be a good alternative to conventional restorations.<sup>6,9</sup> In contrast, after a mean 2.5-year follow-up, the authors concluded that a fiber-reinforced inlay FPD should be only used as a provisional restorations as a result of 72 % cumulative survival rate after 36 months.<sup>10</sup> This reflects that a fiber-reinforced inlay FPD has many factors that need to be improved.

Among the various factors related to the failure of a fiber-reinforced inlay FPD, the effect of the fiber position,<sup>11-13</sup> the fiber composition,<sup>14-16</sup> the length of the missing span,<sup>13</sup> the cementation method of the retainers,<sup>17</sup> the type of cement<sup>18</sup> and the design modification of the pontic FRC framework element<sup>8</sup> have already been reported. In addition, combinations of ceramics and dental composite were used experimentally for a FPD.<sup>19</sup>

Behr et al.<sup>5</sup> compared the two-preparation design forms, of the proximal box (box-shaped vs.

tub-shaped design) and concluded that there was no significant difference in the fracture strength between the two designs. Gohring et al.<sup>17</sup> tested the difference in the cavity bevel design on the marginal quality and Magnè et al.<sup>20</sup> stated that an extension of the preparation for the inlay retainer did not result in an improved stress distribution with a FEM study. Moreover, many researchers reported their own design for fiber-reinforced inlay FPDs. However, from a point of cavity design, their clinical results have not been reported and little information is available on the adequate tooth preparation design related to the connector dimension of the FPD on which the stress is concentrated.

On the other hand, it was reported that the position and thickness of high modulus substrates play a critical role in the fracture strength of the ceramic restorations.<sup>21-24</sup> However, the effect of the core to veneer thickness ratio of the ceromer / FRC on the fracture strength has not been reported.

The aim of this study was to investigate the most fracture resistible thickness combination of ceromer / FRC among the designs by varying the cavity dimensions. Because ceromer / FRC has the characteristics of a greenstick fracture without the catastrophic failure shown in ceramic materials, acoustic emission (AE) analysis was used to investigate the internal crack propagation simultaneously during the test.<sup>25-27</sup>

## MATERIAL AND METHODS

A metal jig, considering the anatomic dimension of the premolars and molars, with a posterior missing span of 11 mm, an isthmus width of 3 mm and a mesiodistal length with either a 4 mm or 6 mm cavity for each retainer was milled (Fig. 1). Two types of metal jigs with 4 mm-deep pulpal walls were fabricated by varying the axial wall height 1 mm or 2 mm. As a result, the thickness

of the retainers in the occlusal cavity ranged from 2 to 4 mm and the thickness of the connectors in the proximal cavity ranged from 3 to 5 mm with various thickness combinations of ceromer / FRC.

With a silicone impression material, 56 polyurethane dies (Modralit-3K, Dreve-GmbH, Unna, Germany) were duplicated from the two types of jigs. The specimens were fabricated with Targis / Vectris system (Ivoclar-Vivadent, Shaan, Liechtenstein). According to the manufacturer's instructions, Vectris (FRC) beams with various connector thicknesses (2 mm (Group 1, 2), 3 mm (group 3-6), 4 mm (group 7)) were con-

structed on these dies. The thickness was adjusted with a carborundum papers from # 800 to # 1000 serially within a 0.1 mm error range with a micrometer (Isomaster, Tesa, Renens, Swiss). After sandblasting, followed by applying a wetting agent, the Vectris beams were veneered with a 1 mm- or 2 mm-thick Targis (ceromer) and were finally cured. The specimens were ground as mentioned earlier.

The fabricated specimens consisted of 7 groups with different ceromer / FRC ratios and different thicknesses of the connectors and isthmus (Table I). The specimens were luted with a Variolink II (Ivoclar-Vivadent, Shaan, Liechtenstein) resin cement on the resin dies and stored at room temperature for 72 hours (Fig. 2).

AE sensors were attached to both sides of the specimens using vacuum grease and subjected to a compressive load until failure at a crosshead speed of 0.5 mm / min. using a 5 mm-diameter steel rod in a universal testing machine. The failure load was recorded with a load-time curve. Simultaneously, the AE signals were detected using a miniature sensor (broadband type model, S9220 by PAC) with a peak sensitivity of -77.5 refs V/mbar and a resonant frequency of 925 kHz. The sensor output was amplified by 60 dB

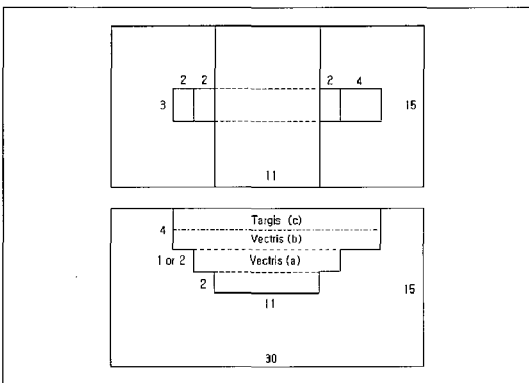


Fig. 1. Dimensions of the inlay FPD and the metal jig.

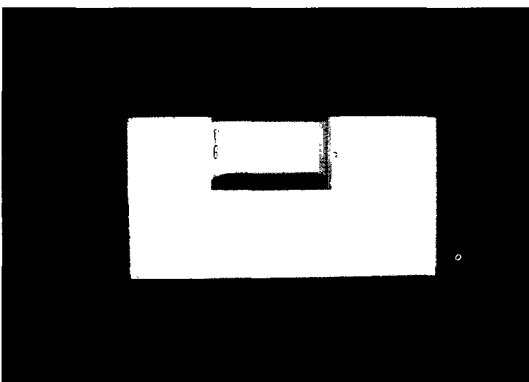


Fig. 2. A luted specimens on the die.

Table I. Thicknesses of components of each group, indicated in Fig. 1

GROUP	VECTRIS thickness, a + b (mm)		TARGIS thickness, c (mm)
	a	b	c
1 (111)	1	1	1
2 (112)	1	1	2
3 (121)	1	2	1
4 (122)	1	2	2
5 (211)	2	1	1
6 (212)	2	1	2
7 (221)	2	2	1

at a preamplifier, which passed through a band-pass filter with a range of 100-1000 kHz. The threshold level was set to 26 dB. The signal was then fed into an AE signal process unit (MISTRAS 2001), where the AE parameters were analyzed using in-built software. Typical AE parameters such as the hit rate and the peak amplitude were investigated to determine the elapsing time.

Failure load 1 (crack initiation point) was considered to be the peak point at which the load decreased and the high amplitude-, AE hit number increased. Failure load 2 (debonding of the interface or FRC fracture initiation point) was considered to be the peak point at which the 10 % load values reduced or the AE hit number increased abruptly despite there being no 10 % loss of load.

Subsequently, the lateral side of the specimens was examined by scanning electron microscopy (SEM) (LEO420, LEO LTD, Cambridge, UK) to investigate the surface crack characteristics at the failure site.

Failure load 1, 2 and the time to failure were analyzed statistically with ANOVA at the 95% confidence level and post-hoc analysis was performed using a Duncan multiple range test. In

order to investigate the structural reliability of each group, Weibull modulus ( $m$ ) and characteristic strength were also compared.

## RESULTS

The AE records or load-time curves for each specimen of group 4, 6, 7 were lost and were not included in the analysis.

The failure loads showed significant differences only in the case of different connector thicknesses (Table II, III,  $P < .05$ ) and no significant differences were found between the same connector thickness groups at both failure load 1 and failure load 2 ( $P > .05$ ). When the connector thickness was the same, there were no significant differences between group 3 with deep pulpal wall and 5 with shallow pulpal wall, and also between group 4 and 6 ( $P > .05$ ). In addition, when the total connector thickness was the same, there were no significant differences between group 2 and groups 3 and 5, and between group 7 and groups 4 and 6, although they have different ceromer / FRC ratios ( $P > .05$ ).

A similar phenomenon was also observed in the characteristic strength values. If the groups have

**Table II.** Duncan's multiple range test of Load 1 ( $\alpha = .05$ )

GROUP	N	GROUPING (N)		
		1	2	3
1 (111)	8	215.96		
2 (112)	8		329.26	
3 (121)	8		375.53	
5 (211)	8		379.45	
7 (221)	7			471.39
4 (122)	7			477.41
6 (212)	7			488.37
<i>p value</i>		1.000	0.239	0.703

**Table III.** Duncan's multiple range test of Load 2 ( $\alpha = .05$ )

GROUP	N	GROUPING (N)		
		1	2	3
1 (111)	8	283.46		
2 (112)	8		399.98	
5 (211)	8		414.43	
3 (121)	8		417.24	
4 (122)	7			532.43
7 (221)	7			535.35
6 (212)	7			541.89
<i>p value</i>		1.000	0.572	0.802

the same connector thickness, the characteristic strengths were very similar each other (Table IV). However, time to failure of each group showed different patterns, until failure load 1. Groups 1 and 2 took  $52.88 \pm 9.01$  seconds and  $52.75 \pm 4.20$  seconds, respectively, and these groups were significantly different from group 7, which took  $69.43 \pm 15.67$  seconds ( $P < .05$ ). The 5 mm-thick connector groups (group 4, 6, 7) showed very high Weibull modulus ( $m$ ) values (Table IV, Fig. 3, 4).

The AE signals appeared just after loading, and particularly in the group 1 and 2, an abundant

increase in the initial AE hit numbers and a decrease in the load, were recorded (Fig. 5). The AE hit numbers correlated well with the load-time curve and the load decrease point was the releasing time of the high amplitude AE. In the later stages of the load-time curve, the high amplitude AE hit numbers representing the fracture of the FRC Vectris substrate were recorded. The AE hit numbers detected at the short retainer (4 mm) were similar to those of the long retainer (6 mm).

In the SEM, a crack was initiated at the interface of the Targis / Vectris and propagated to the

**Table IV.** Weibull modulus  $m$  and characteristic strength  $\sigma_0$  (N)

GROUP	Load 1		Load 2	
	Weibull modulus $m$	Characteristic strength $\sigma_0$ (N)	Weibull modulus $m$	Characteristic strength $\sigma_0$ (N)
1 (111)	9.97	227.03	5.04	308.60
2 (112)	3.47	366.12	4.84	436.43
3 (121)	6.94	401.63	8.07	442.88
4 (122)	9.91	502.02	14.82	551.58
5 (211)	4.95	413.53	5.54	448.71
6 (212)	11.00	511.34	42.11	549.11
7 (221)	7.38	502.57	16.15	553.14

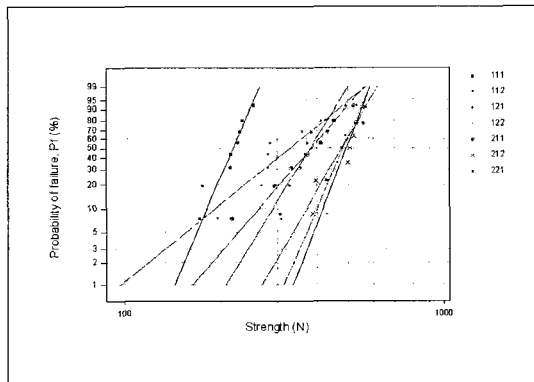


**Fig. 3.** Weibull plots of failure strength at failure load 1. Steeper slope indicated more uniform strength.

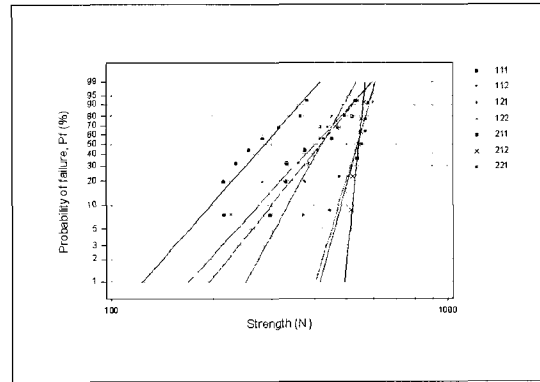


**Fig. 4.** Weibull plots of failure strength at failure load 2. Steeper slope indicated more uniform strength.

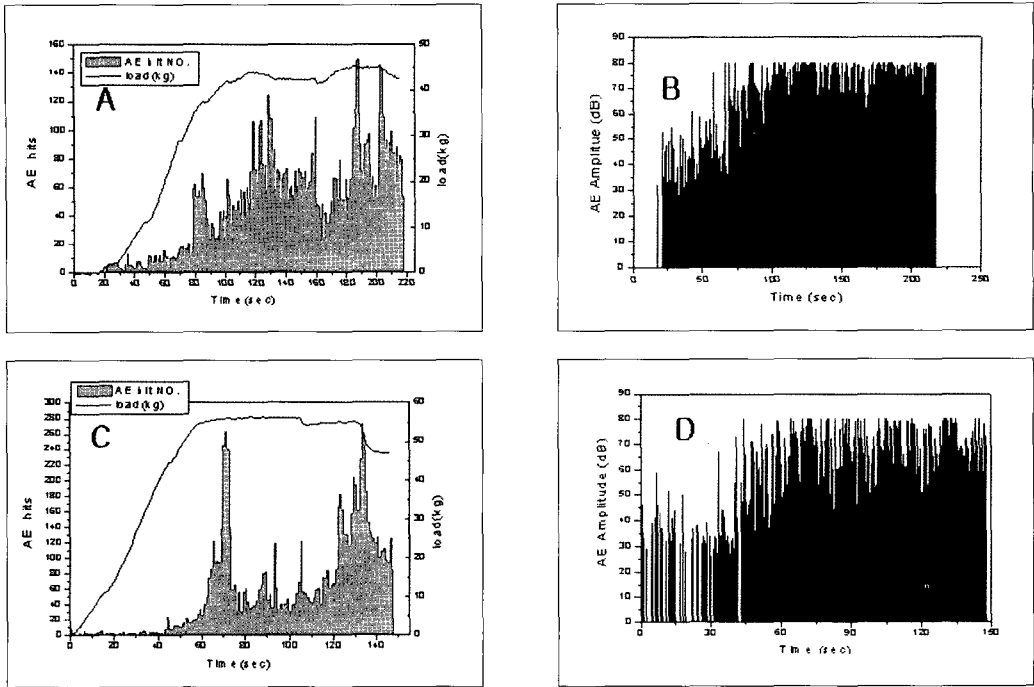


Fig. 5. Load-time curve and number of AE counts of group 2 (A), and group 4 (C). AE amplitude of group 2 (B), and group 4(D).

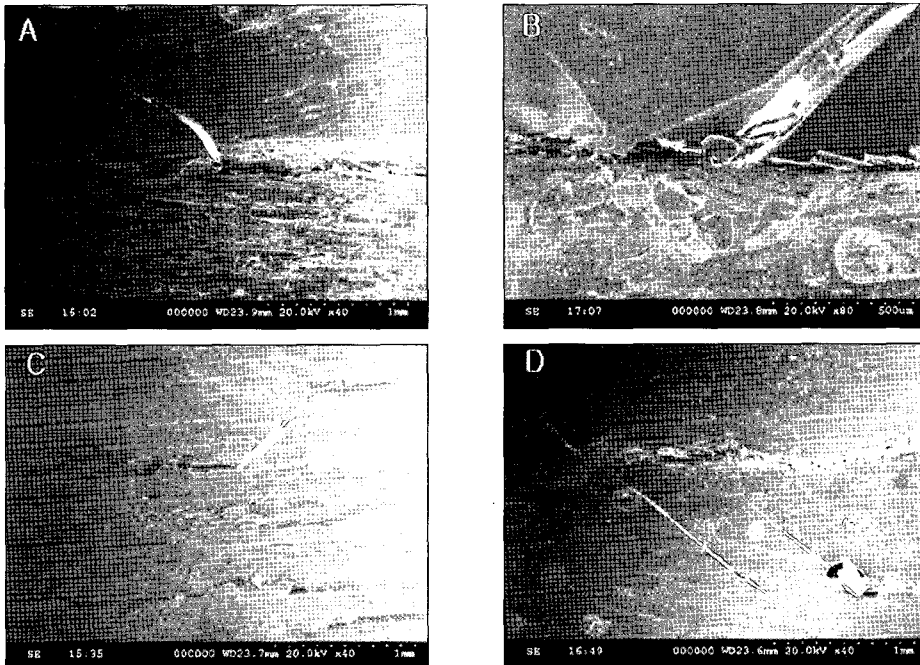


Fig. 6. SEM views of Targis / Vectris interfaces. A, Crack initiation at the interface and propagation to the Targis layer. B, Debonding of the Targis from the Vectris layer. C, Delamination of the Vectris layer. D, Crack propagation within the Vectris layer.

Targis layer (Fig. 6). In addition, the crack advanced along the interface and evoked the debonding of Targis from the Vectris layer. The cracks parallel to the fiber direction within the Vectris layer was also observed. Fiber fracture of FRC was demonstrated at the interface.

## DISCUSSION

The failure strength of the inlay FPDs made of ceromer / FRC was recorded in order to investigate the most resistant dimension of inlay FPD with various thicknesses combinations. As a result, the depth of the proximal box i.e. the total thickness of the connectors at the gingival wall correlated with the fracture resistance regardless of both the ceromer / FRC ratio and the depth of the pulpal wall.

With ceramics, the connector dimensions allowed for premolars are  $4 \times 5$  mm and need to be at least  $4 \times 4$  mm.<sup>28-31</sup> In contrast, little is known regarding the effect of ceromer / FRC FPD connector dimensions. Behr et al.<sup>5</sup> reported 700 N failure strength of fiber-reinforced inlay FPDs with an isthmus width of 3 mm and a proximal depth of 4 mm, and Rosentritt et al.<sup>32</sup> also reported failure strength of 830-940 N using  $4 \times 4$  mm connectors. Gohring et al.<sup>17</sup> reported  $5 \times 4$  mm cavity dimension in molars.

However, in most studies, the cavity design appears insufficient. The widths of the isthmus were 1.5-2.0 mm in the premolars and 2.5-3.0 mm in the molars<sup>9,33,34</sup> and the depths of the occlusal cavity were 1.5 mm,<sup>35</sup> 2-2.5 mm,<sup>9</sup> and 2.5-3.0 mm<sup>9,33</sup> In case of the proximal box preparation, the optimal dimension<sup>35</sup> or a not fully extended preparation<sup>4</sup> has been recommended. However, in this study, the failure strength of the fiber-reinforced inlay FPDs were affected by the total thickness of connectors rather than by the ceromer / FRC ratio or the occlusal retainer thickness. Therefore, as seen in the ceramic mate-

rial, it is important to prepare the adequate depth of the proximal box.

Wakabayashi et al.<sup>23</sup> stated that the failure loads increased significantly as the core / veneer ratio was increased and concluded that the core / veneer thickness ratio appeared to be the dominant factor that controls the failure initiation site in the bilayer ceramic restorations. This is in contrast to this study where variations of the ceromer / FRC ratio had no significant effect on the failure loads and the crack initiation site.

In the FEM simulation study, Magne et al.<sup>20</sup> reported that tensile forces in the interfaces of the inlay FPD were high at the gingivoaxial walls of the interproximal box, but the gingivoaxial wall height variation did not have any effect in this study. Although a shallow occlusal cavity makes a thin occlusal retainer and a high gingivoaxial wall, the failure loads were not significantly different.

Magne et al.<sup>20</sup> also reported that an extension of the preparation did not result in an improved stress distribution. This was similar to that reported by Loose et al.<sup>36</sup> who indicated negative effects on the join areas furthest away from the center of the fiber-reinforced inlay FPD. This could be explained by the high flexibility of the ceromer / FRC, but a too short retainer could be the cause of a weak bonding strength. In this study, a short and long retainer showed a similar failure pattern and a similar AE hit number. However, more research on the effect of length of the retainer will be needed.

The Weibull modulus ( $m$ ) and the characteristic strength are statistical parameters representing the structural reliability.<sup>21</sup> A high Weibull modulus value indicates a smaller error range for a clinical study. The characteristic strength represents the 63.21 % of the strength distribution corresponding to a mean value for a material. In this study, group 4, 6, 7, which had 5 mm-thick connectors, showed  $m$  values in the range of 14-42 at failure load 2 over the general range of ceramic

materials. This means that a fiber-reinforced inlay FPD with 5 mm-thick connectors is a clinically reliable restoration with a high success rate. In contrast, group 2 (112) had very low Weibull modulus values. This means there is a larger strength distribution in the group 2 specimens. Moreover, a shorter time until failure load 1 of group 1 and 2 means that the 2 mm-thick FRC groups (group 1, 2) made rapid crack propagation when compared to 4 mm-thick FRC group.<sup>7</sup> These were also accordance with the pattern of the load-time curve and the AE hit numbers. Therefore, clinicians should be cautious when using connectors including those with a FRC thickness 2 mm or less, although this study suggests that the total thickness of the connectors is a dominant factor.

The actual failure point in the ceromer / FRC restorations might be controversial. In previous studies, the failure of a ceromer / FRC restoration was set to a 10 % loss of the maximum load or a point where there is a sharp decrease in the maximum load, and bending at failure loads were either 0.9-1.2 mm or 2 mm.<sup>5</sup> Although this amount of bending reflects the ceromer / FRC flexibility, it is difficult to reproduce this in the mouth without debonding the retainers. Moreover, as shown in figure 6, fracture of a ceromer / FRC restoration was not a catastrophic fracture but a greenstick fracture. Therefore, a comparison of the failure load at the maximum peak stress point is an incorrect method for estimating the failure of a ceromer / FRC material. In this study, the failure load was set to a point where a decrease in the load coincides with an increase in the high amplitude AE hit numbers.

The AE is the elastic wave that is spontaneously released by plastic deformation, crack growth or debonding and fracture of the fillers or fibers in a ceromer / FRC material. This study showed that the low amplitude AE events representing the separation of the filler particles from the matrix<sup>26</sup>

were released immediately after loading, and the high amplitude AE events representing the crack initiation were also released earlier than at the maximum peak stress. In addition, even at the failure load 2 peak stress, which is believed to be a starting point for interfacial crack propagation or FRC fracture, there were no 10 % loss of load in many cases. A sharp decrease in the load was shown even after the FPD was bent by 1 mm. However, with an evaluation of the AE hit numbers, this point was later than the debonding point of the ceromer from the FRC, which is believed to be a 'real' failure. In this study, the application of AE analysis methods can be used to evaluate the fracture behavior and analyze the precise fracture point. Therefore, predicting the failure of a fiber-reinforced inlay FPD should be supplemented with an AE analysis to detect the microfracture and initial internal crack propagation.

SEM showed that the fracture was initiated from the interface and propagated into the Targis layer regardless of the change in the Targis / Vectris ratio. The debonding of the Targis from the Vectris and debonding within the Vectris layers followed this fracture. This is accordance with the reports showing that the success of a system depends on the cohesiveness between the fibers and the surrounding resin matrix.<sup>12,20</sup>

In the molar areas, the maximum bite force was known as 390-800 N.<sup>37</sup> This study showed that the failure loads were lower than those of previous studies and these values are insufficient to restore posterior missing tooth. This is because the Vectris of an inlay FPD was not covered with Targis as it is in clinical situations. Therefore, these results cannot be directly extrapolated to the clinical failure load. Another explanation is to apply a strict failure point using AE analysis. Although resin dies with a similar elastic modulus of the dentin were used in this study, bonding to these dies could have the differences of fracture strength, bond strength and debonding pattern when com-



pared to bonding to natural teeth.

Another limitation of this study was that the failure strength was recorded under the static load without a fatigue phenomenon induced by a dynamic load and a wet environment. Despite the many advantages of ceromer / FRC materials, there needs to be some caution when considering of fiber-reinforced inlay FPDs for clinical applications. Further research into the cavity design and dimension will be needed in order to reduce the relatively high failure in a fiber-reinforced inlay FPD.

## CONCLUSION

Within the limitations of this study, the failure loads showed significant differences only in the case of different connector thicknesses, and no significant differences were found between the same connector thickness groups. When the connector thickness was the same, there were no significant differences between the groups with different occlusal pulpal wall depths and between the groups with different ceromer / FRC ratios. Fiber-reinforced inlay FPD with 5 mm-thick connectors showed higher Weibull modulus ( $m$ ) values, which could be used as a clinically reliable restoration with a high success rate. Due to their rapid crack propagations, some caution should be taken when using connectors including FRC with a thickness 2 mm or less for restoring posterior inlay FPDs, even though they have a sufficient thickness. SEM showed that fracture initiated from the interface and propagated into the Targis layer regardless of the change in the Targis / Vectris ratio. The application of an AE analysis method for the fiber-reinforced inlay FPDs helped to evaluate the fracture behavior and to analyze the precise fracture point.

## REFERENCES

1. Serdar CH, Ozturk B. Posterior bridges retained by resin-bonded cast metal inlay retainers: a report of 60 cases followed for 6 years. *J Oral Rehabil* 1997;24:697-704.
2. Fradeani M, Barducci G. Lithium disilicate glass-ceramic restorations: indications and guidelines. In: *Quintessence of dental technology*. Chicago; Quintessence; 2000. p. 51-62.
3. Edelhoff D, Spiekermann H, Yildirim M. Metal-free inlay-retained fixed partial dentures. *Quintessence Int* 2001;32:269-281.
4. Freilich MA, Karmarker AC, Burstone CJ, Goldberg AJ. Development and clinical applications of a light-polymerized fiber-reinforcement composite. *J Prosthet Dent* 1998;80:311-318.
5. Behr M, Rosentritt M, Leibrock A, Schneider-Feyrer S, Handel G. In-vitro study of fracture strength and marginal adaptation of fibre-reinforced adhesive fixed partial inlay dentures. *J Dent* 1999;27:163-168.
6. Göhring TN, Mormann WH, Lutz F. Clinical and scanning electron microscopic evaluation of fiber-reinforced inlay fixed partial dentures; preliminary results after one year. *J Prosthet Dent* 1999;82:662-668.
7. Vallittu PK, Sevelius C. Resin-bonded, glass fiber-reinforced composite fixed partial dentures: a clinical study. *J Prosthet Dent* 2000;84:413-418.
8. Monaco C, Ferrari M, Micel GP, Scotti R. Clinical evaluation of fiber-reinforced composite inlay FPDs. *Int J Prosthodont* 2003;16:319-325.
9. Iglesia-Puig MA, Arellano-Cabornero A. Inlay fixed partial denture as a conservative approach for restoring posterior missing teeth: a clinical report. *J Prosthet Dent* 2003;89:443-445.
10. Behr M, Rosentritt M, Handel G. Fiber-reinforced composite crowns and FPDs: a clinical report. *Int J Prosthodont* 2003;16:239-243.
11. Ellakwa AE, Shortall AC, Shehata MK, Marquis PM. The influence of fibre replacement and position on the efficiency of reinforcement of fibre reinforced composite bridge work. *J Oral Rehabil* 2001;28:785-791.
12. Ellakwa AE, Shortall AC, Marquis PM. Influence of fibre position on the flexural properties and strain energy of a fibre-reinforced composite. *J Oral Rehabil* 2003;30:679-682.
13. Nohrström TJ, Vallittu PK, Yli-Urpo A. The effect of placement and quantity of glass fibers on the fracture resistance of interim fixed partial dentures. *Int J Prosthodont* 2000;13:72-78.
14. Bae JM, Kim KN, Hattori M, Hasegawa K, Yoshinari M, Kawada E, Oda Y. The flexural properties of fiber-reinforced composite with light-polymerized polymer matrix. *Int J Prosthodont* 2001;14:33-39.

15. Vallittu PK. The effect of glass fiber reinforcement on the fracture resistance of a provisional fixed partial denture. *J Prosthet Dent* 1998;79:125-130.
16. Kolbeck C, Rosentritt M, Behr M, Lang R, Handel G. In vitro study of fracture strength and marginal adaptation of polyethylene-fibre-reinforced-composite versus glass-fibre-reinforced-composite fixed partial dentures. *J Oral Rehabil* 2002;29:668-674.
17. Gohring TN, Peters OA, Lutz F. Marginal adaptation of inlay-retained adhesive fixed partial dentures after mechanical and thermal stress: an in vitro study. *J Prosthet Dent* 2001;86:81-92.
18. Behr M, Rosentritt M, Ledwinsky E, Handel G. Fracture resistance and marginal adaptation of conventionally cemented fiber-reinforcement composite three-unit FPDs. *Int J Prosthodont* 2002;15:467-472.
19. Rosentritt M, Behr M, Handel G. Fixed partial dentures: all-ceramics, fibre-reinforced composites and experimental systems. *J Oral Rehabil* 2003;30:873-877.
20. Magne P, Belser UC, Krejci I. Stress distribution of inlay-anchored adhesive fixed partial dentures: a finite element analysis of the influence of restorative materials and abutment preparation design. *J Prosthet Dent* 2002;87:516-527.
21. Bonna AD, Anusavice KJ, DeHoff PH. Weibull analysis and flexural strength of hot-pressed core and veneered ceramic structures. *Dent Mater* 2003;19:662-669.
22. White SN, Caputo AA, Vidjak FMA, Seghi RR. Moduli of rupture of layered dental ceramics. *Dent Mater* 1994;10:52-58.
23. Wakabayashi N, Anusavice KJ. Crack initiation modes in bilayered alumina/porcelain disks as a function of core/veneer thickness ratio and supporting substrate stiffness. *J Dent Res* 2000;79:1398-1404.
24. Caputo AA, Li ZC, Zhao XY. Modulus of rupture of the Procera All-Ceramic system. *J Esthet Dent* 1996;8:120-126.
25. Kim KH, Okuno O. Microfracture behavior of composite resins containing irregular-shaped fillers. *J Oral Rehabil* 2002;29:1153-1159.
26. Kim KH, Kim YB, Okuno O. Microfracture mechanics of composite resins containing prepolymerized particle fillers. *Dent Mater* 2000;19:22-23.
27. Vallittu PK. Use of woven glass failures to reinforce a composite veneer. A fracture resistance and acoustic emission study. *J Oral Rehabil* 2002;29:423-429.
28. Sorensen JA, Cruz M, Mito W, Raffeiner O, Meredith HR, Foser HP. A clinical investigation on three-unit fixed partial dentures fabricated with a lithium disilicate glass-ceramic. *Pract Periodont Aesthet Dent* 1998;11:95-106.
29. IPS Empress 2 Instruction / work manual. Ivoclar North America Inc, July 1999.
30. Sorensen JA. The IPS Empress 2 system: defining the possibilities. In: *Quintessence of dental technology*. Chicago;Quintessence; 1999. p. 153-163.
31. Moto W, Sorensen JA. Fabrication of fixed partial dentures with Empress 2. In: *Quintessence of dental technology*. Chicago;Quintessence; 1999. p. 164-169.
32. Rosentritt M, Behr M, Kolbeck C, Handel G. In vitro repair of three-unit fiber-reinforced composite FPDs. *Int J Prosthodont* 2001;14:344-349.
33. Shannon A. Fiber-reinforced composite bridge: inlay-to-inlay technique. *Dent Today* 1997;Nov:48-53.
34. Krejci I, Boretti R, Giezendanner P, Lutz F. Adhesive crowns and fixed partial dentures fabricated of ceromer/FRC: clinical and laboratory procedures. *Pract Periodont Aesthet Dent* 1998;10:487-498.
35. Bartsch F. Fiber-reinforced inlay bridges: Guidelines for clinical and laboratory fabrication of Targis/Vectris metal-free inlay bridges. In: *Quintessence of dental technology*. Chicago; Quintessence;2000. p. 117-138.
36. Loose M, Rosentritt M, Leibrock A, Behr M, Handel G. In vitro study of fracture strength and marginal adaptation of fibre-reinforced-composite versus all ceramic fixed partial dentures. *Eur J Prosthodont Rest Dent* 1998;6:55-62.
37. Craig RG, ed. *Restorative dental materials*. 6th ed. St. Louis;Mosby; 1980. p. 60-61.

*Reprint request to:*

YANG-JIN YI, D.D.S., M.S.D., PH.D.  
 DEPARTMENT OF PROSTHODONTICS, COLLEGE OF DENTISTRY,  
 KANGNUNG NATIONAL UNIVERSITY  
 123 JIBYUN-DONG, KANGNUNG, 210-702, KOREA  
 navydent@kangnung.ac.kr

*2003 Annual Fall Scientific Meeting of  
The Korean Academy of Prosthodontics*

November 28-29, 2003, Seoul, Korea



Fig 1. Representatives general meeting at Jamsil Lotte Hotel.



Fig 2. Officers and directors of KAP with invited speakers after scientific meeting.



Fig 3. Welcome reception for invited speakers, KAP officers and directors by the President Dae-Gyun Choi.

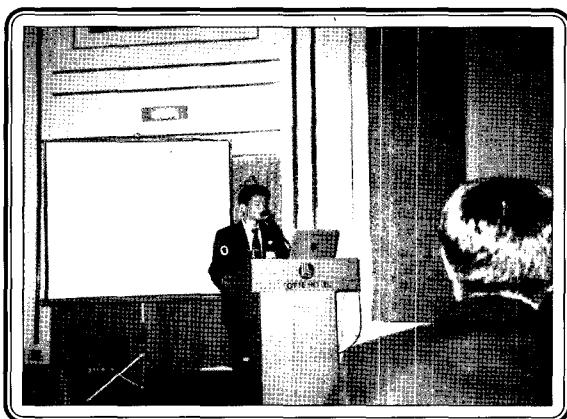


Fig 4. Oral Presentation

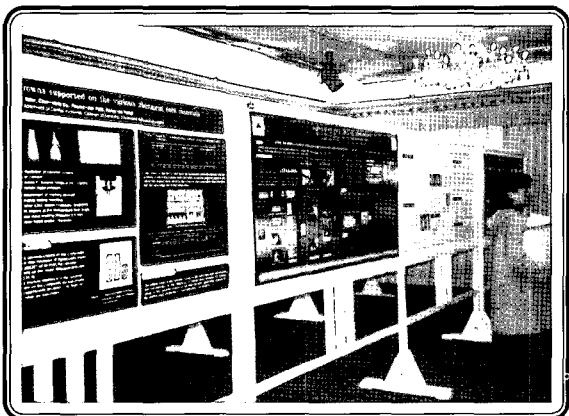


Fig 5. Poster presentation



Fig 6. Invited speaker (Dr. Yoshinobu Maeda)

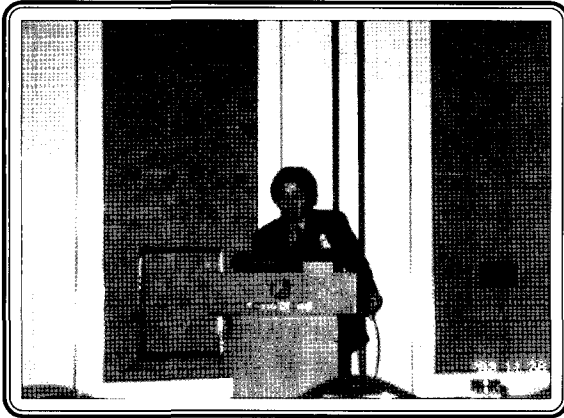


Fig 7. Invited speaker (Dr. Joseph Y Kan)



Fig 8. New academy certified Prosthodontists



Fig 9. Exhibition hall

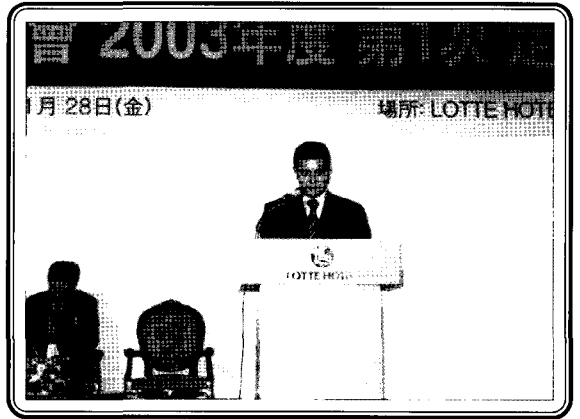


Fig 10. New president of the Korean Academy of Prosthodontics (2003.12-2005.11)